

# Modified Natural Commutated Switching Technique for HF Link Inverter

C. L. Nge and Z. Salam  
Department of Energy Conversion  
Faculty of Electrical Engineering,  
Universiti Teknologi Malaysia,  
81310 UTM Skudai, Johor Bahru, MALAYSIA  
E-Mail: zainals@fke.utm.my

## Acknowledgements

This work was supported by the Intensification of Research in Priority Areas grant from the Ministry of Science, Technology and the Environment, Malaysia. The authors gratefully acknowledge the Universiti Teknologi Malaysia for providing excellent experimental facilities.

## Keywords

Soft switching, voltage source inverters, switched-mode power supply

## Abstract

This paper proposes a modified natural commutated control HF link inverter topology that consists of a center-tapped transformer and three bidirectional switching arms on the transformer secondary side. The topology is able to simultaneously utilize unipolar SPWM control scheme and natural commutation technique. The conversion efficiency is inherently high due to the existence of freewheeling periods per switching cycle and the utilization of zero current switching (ZCS) and zero voltage switching (ZVS) operation. Moreover, with minimum number of power switches at cycloconverter stage, the conduction loss can be further reduced. The operating principles of the proposed topology and switching technique are verified by experimental results.

## Introduction

In order to reduce the size and weight of the transformer, high-frequency (HF) link power conversion systems have been examined [1-5]. This type of converter normally has two conversion stages. There are two main circuits for the HF link inverter; namely the “dc-dc converter” type” and the “cycloconverter” type. HF link inverters with cycloconverter at the output stage of the system have a merit of bidirectional power flow. However, HF link cycloconverter type inverters that employ SPWM technique to reduce the output voltage harmonic components, suffer from inherent problem of voltage surge across transformer secondary side main switches. It is due to forced interruption of continuous current flow in leakage inductances of HF transformer by cycloconverter stage self turn-off devices. To solve this problem, several voltage clamp circuits have been developed [6-7].

Fig. 2 shows the widely known phase angle control HF link dc/ac converter that utilizes natural commutation technique to avoid forced interruption of current flow in leakage inductances and results in a reduced voltage spike [8]. This non-resonant approach has the advantage of low circuit complexity and no increased device voltage or current ratings. The topology consists of four pairs of bidirectional switching arms at the cycloconverter stage. This converter system must employ bipolar SPWM switching scheme to avoid occurrence of voltage surge.

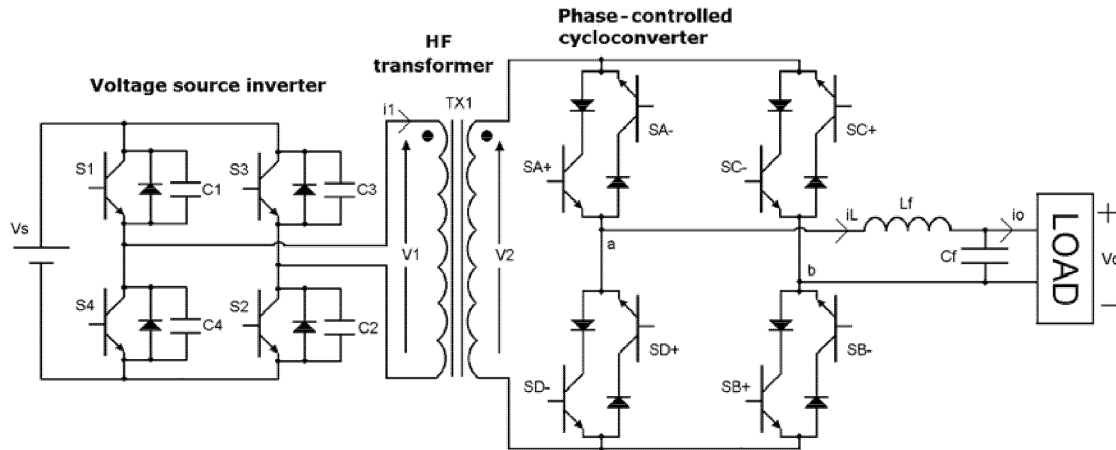


Fig. 1: Natural commutated phase angle control HF link inverter

The authors proposed an alternative natural commutated control HF link inverter topology that consists of a center-tapped transformer and three bidirectional switching arms on transformer secondary side. This topology is able to simultaneously utilize unipolar SPWM switching scheme and natural commutation technique.

## Operating Principles

The proposed circuit configuration is shown in Fig. 2. It is a two-stage cycloconverter type HF link inverter with single-phase output stage. This circuit topology enables bidirectional power flow. Therefore, it is suitable for renewable energy source systems. The primary side of the HF transformer terminals is connected to the voltage source inverter. The bridge inverter generates square wave constant frequency output. The waveform consists of only high frequency harmonics so that a small sized high frequency transformer is allowed. The inverter operates with ZVS condition because of the existence of natural commutation phenomena at cycloconverter stage.

The cycloconverter stage has three bidirectional switching arms. The first switching arm  $SX$  consists of transistors  $MX+$ ,  $MX-$  and diodes  $DX+$ ,  $DX-$ . The second switching arm  $SY$  consists of transistors  $MY+$ ,  $MY-$  and diodes  $DY+$ ,  $DY-$ . These two switch sets are the powering switching arms that transfer instantaneous power from the dc voltage source to the load. The third switching arm  $SZ$ , which consists of transistors  $MZ+$ ,  $MZ-$  and diodes  $DZ+$ ,  $DZ-$  provides freewheeling path for the output current when the output voltage is clamped to zero. For the control of secondary cycloconverter stage, edge aligned unipolar PWM switching scheme is applied. Since the converter uses gate turn-off devices to operate in natural commutation mode, overlap periods  $t_{c1}$  and  $t_{c2}$  are added to the control pulse pattern. The utilization of natural commutation technique allows total soft-switched operation at the inverter and cycloconverter stage. The soft switching mechanism and commutation phenomena are discussed in detail later.

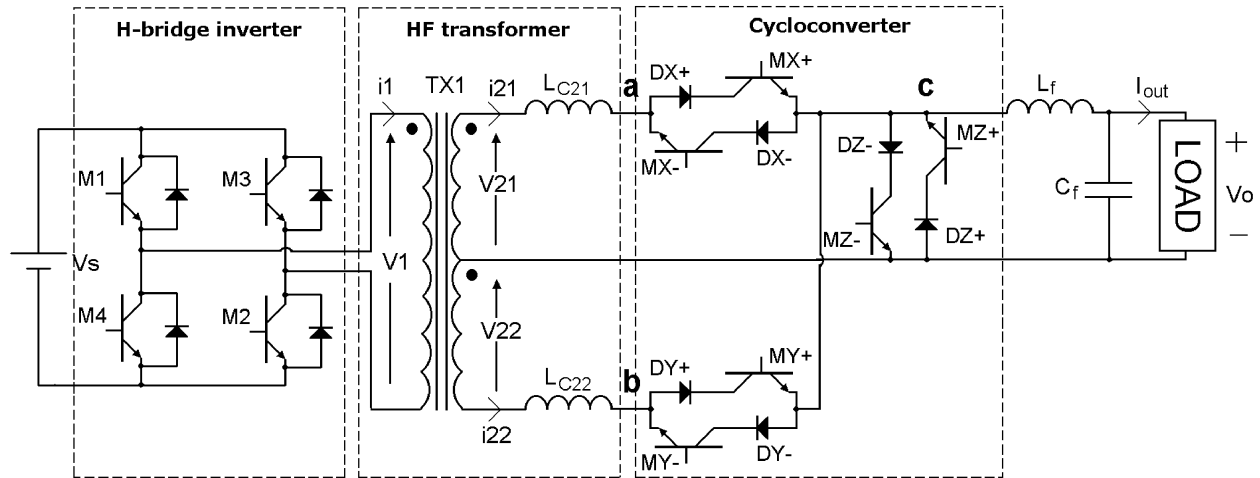


Fig. 2: Proposed natural commutated unipolar SPWM control HF link inverter

### Control Signal Timings

Fig. 3 shows the basic control signal timings for both inverter and cycloconverter stages. The control signals are synchronized to the same reference oscillator. At the inverter stage dead time  $t_d$  is added to every switching transition to avoid cross conduction. For the cycloconverter stage, the switching signals are obtained by comparing the modulating waveform with the saw-tooth carrier waveform. Switching arm  $SX$  turns on when the output voltage follows HF transformer output voltage, while switching arm  $SY$  turns on when the output voltage reverses HF transformer output voltage. Overlap period  $t_{c1}$  is set at switching transition from freewheeling switching arm to powering switching arms while  $t_{c2}$  is set at switching transition from powering switching to freewheeling switching arm. The direction of output current flow determines the switching of “+” and “-” groups at cycloconverter stage.

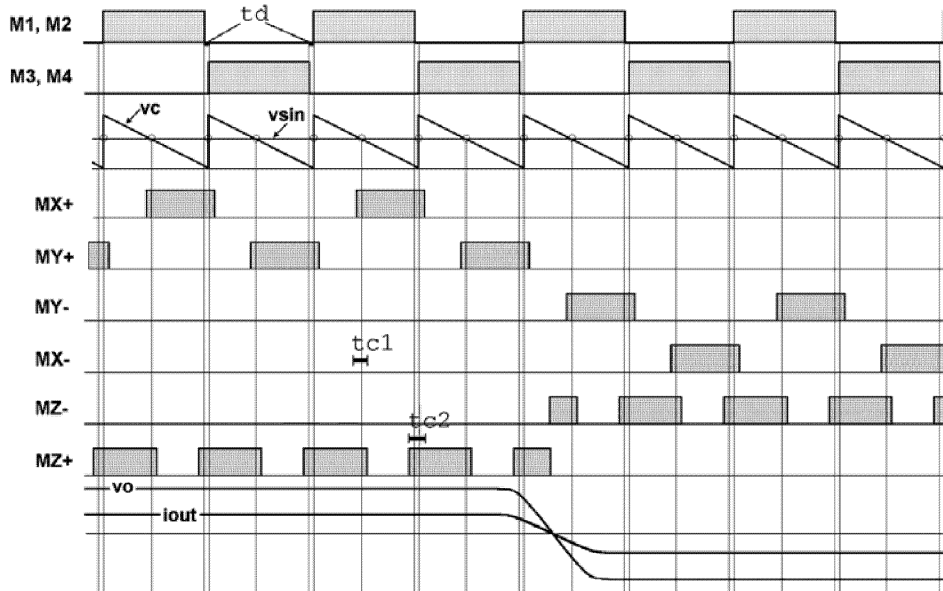


Fig. 3: Control signal timings

## Principles of Soft Switching Operation

Assume positive voltage across transformer primary side winding with output voltage  $v_o$  and output current  $I_{out}$  positive. Figure 4 depicts the current flow path for natural commutation at cycloconverter and forced commutation at H-bridge inverter. The natural commutation mechanism at cycloconverter stage during overlap period  $t_{cl}$  can be explained by referring to Fig. 5a. Assume positive voltage across transformer primary side winding with output voltage  $v_o$  and output current  $I_{out}$  positive. Immediately prior to  $MX+$  turns on, the load current freewheels through  $DZ+$  and  $MZ+$ . When  $MX+$  turns on at zero current,  $DX+$  is forward biased and is also turned on. Considering commutation from switching arm  $SZ$  to  $SX$  between  $t_1$  and  $t_2$ , and that the load current  $I_{out}$  is assumed constant, the following equations are written:

$$v_{21} = L_{c21} \frac{di_{21}}{dt} + v_a \quad (1)$$

$$i_{21} + i_{MZ+} = I_{out} \quad (2)$$

Hence,

$$\frac{di_{21}}{dt} + \frac{di_{MZ+}}{dt} = 0 \quad (3)$$

Given that at time  $t_1$ ,

$$v_{21}(t_1) = V_p = \frac{V_s}{(N1/N2)} \quad (4)$$

where  $N1/N2$  is transformer turns ratio. Also,

$$v_a(t_1) = 0 \quad (5)$$

Combining equations (1) and (2) yields

$$\frac{di_{21}}{dt} = -\frac{di_{MZ+}}{dt} = +\frac{V_p}{L_{C1}} \quad (6)$$

When freewheeling current  $i_{MZ+}$  reaches zero, commutation process is completed. At time  $t_2$  transistor  $MZ+$  is turned off at zero current, and results in no voltage surge. From  $t_2$  onwards, voltage at point  $c$  rises to  $+V_p$  while instantaneous power transfers from dc source to the load.

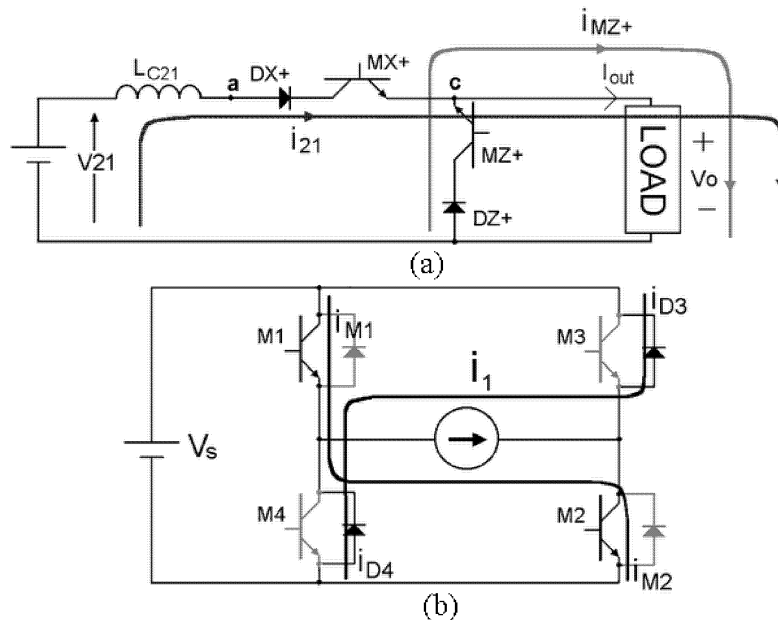


Fig. 4: Current flow path for a) natural commutation b) forced commutation

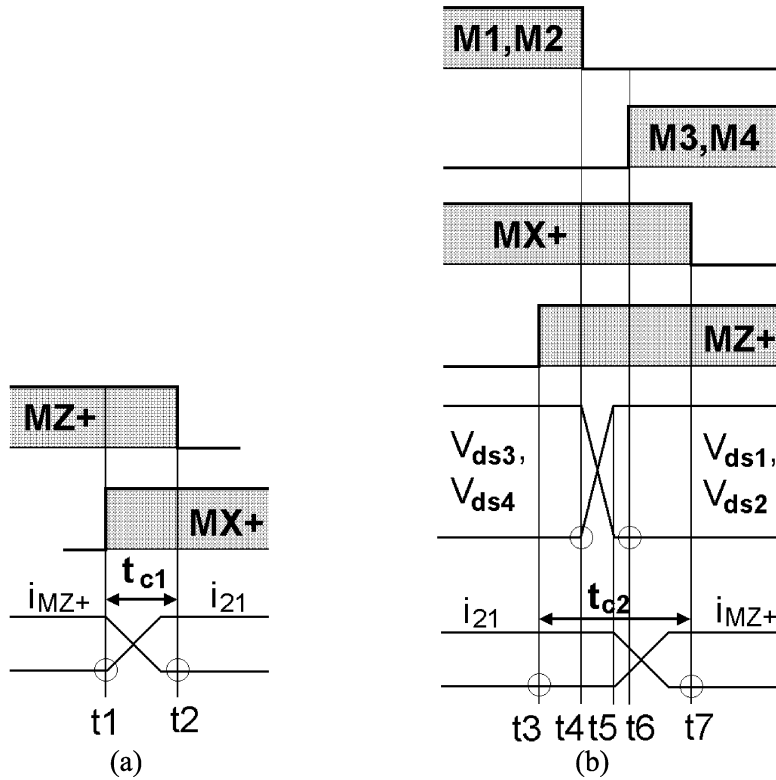


Fig.5: Principle of soft switching operation during overlap period a)  $t_{c1}$  and b)  $t_{c2}$

The ZVS operation at inverter stage, ZCS operation and the natural commutation mechanism at cycloconverter stage during overlap period  $t_{c2}$  are explained in detail in Fig. 5b. Immediately before  $MZ+$  turns on, instantaneous power transfers from dc source to the load through transistors  $M1$ ,  $M2$ , and switching arm  $SX$ . At time  $t_3$ ,  $MZ+$  is turned on at zero current, since that  $DZ+$  is reversed biased and voltage at point  $c$  is clamped to  $+V_p$ .  $M1$  and  $M2$  turn off at zero voltage at time  $t_4$ , forcing  $i_l$  to commute from  $M1$  and  $M2$  to anti-parallel diodes of  $M3$  and  $M4$ . As a result, output capacitances of  $M3$  and  $M4$  are discharged; voltages  $V_{ds3}$  and  $V_{ds4}$  fall to zero while  $V_{ds1}$  and  $V_{ds2}$  rise to  $+V_S$ . At time  $t_5$ ,  $v_l$  is inverted to  $-V_S$  so that  $v_{21}$  equals to  $-V_p$ .  $DZ+$  is forward biased and voltage at point  $c$  is held to zero. At time  $t_6$ ,  $M3$  and  $M4$  turn on at zero voltage. Between time  $t_4$  and  $t_6$ , is dead time  $t_d$ , which is set to avoid cross conduction and also enable ZVS operation. Load current  $I_{out}$  commutate from switching arm  $SX$  to  $SZ$  between  $t_5$  and  $t_7$  with the following equation:

$$\frac{di_{21}}{dt} = -\frac{di_{MZ+}}{dt} = -\frac{V_p}{L_{c1}} \quad (7)$$

When transformer current  $i_{c21}$  reaches zero, commutation process is completed. At time  $t_7$  transistor  $MX+$  is turned off at zero current, and results in no voltage surge. From  $t_7$  onwards, load current  $I_{out}$  freewheels through switching arm  $Z$  while instantaneous power is supplied from  $LC$  filter to the load.

Since the converter control signals are periodical symmetry, soft switching operations and natural commutation mechanisms during switching transitions between switching arms  $SY$  and  $SZ$  are similar to operations as explained above. Therefore, every switching operation at the both conversion stages is performed with soft switching manner.

## Results and Analysis

The experimental output waveforms are as shown in Fig. 6. This verifies that the proposed topology is able to generate output voltage of  $120V_{rms}$  and  $240V_{rms}$ . The primary stage uses IRG4PC50UD, while the secondary stage uses IRG4PH50U and 60EPF12 from International Rectifier. The HF transformer is constructed on Ferrite core ETD59 from Ferroxcube. With output filter  $L_f = 16mH$  and  $C_f = 2.2\mu F$ , THD less than 2.5% is achieved for resistive load ranging from  $32\Omega$  to  $250\Omega$ .

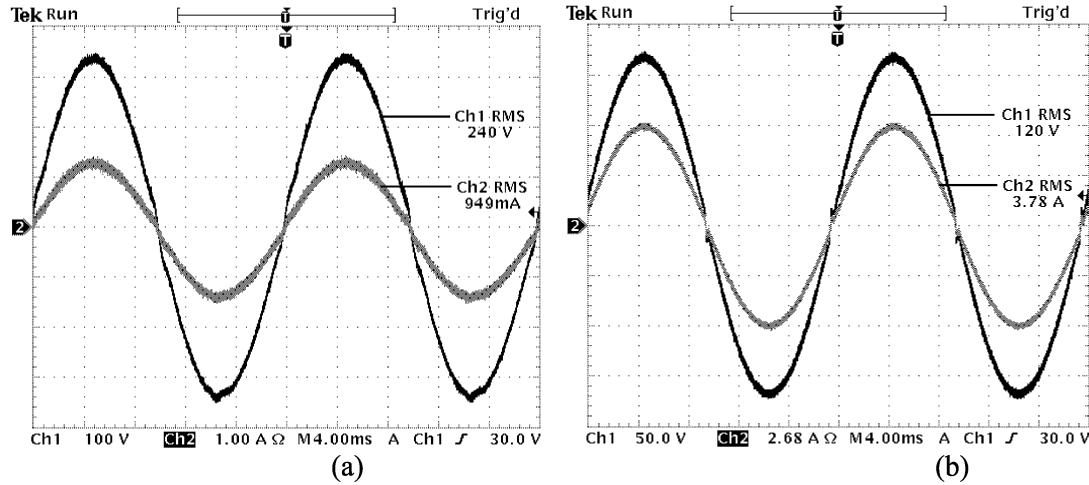


Fig. 6: Experimental results of output voltage (a)  $240V_{rms}$  and (b)  $120V_{rms}$

The operating waveforms at both bridge inverter and cycloconverter stage are shown in Fig. 7. The output voltage at node  $c$  is unipolar. The extended waveforms in Fig. 8 confirm that soft-switching operation is achieved at both primary and secondary stage. Voltage oscillations occur during dead time due to diode reverse-recovery characteristic.

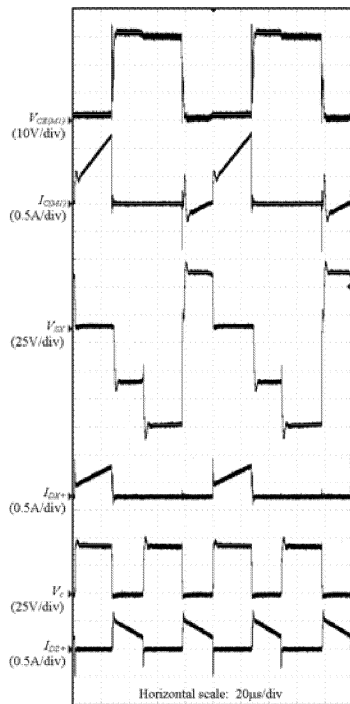


Fig. 7: Overall efficiency versus output power

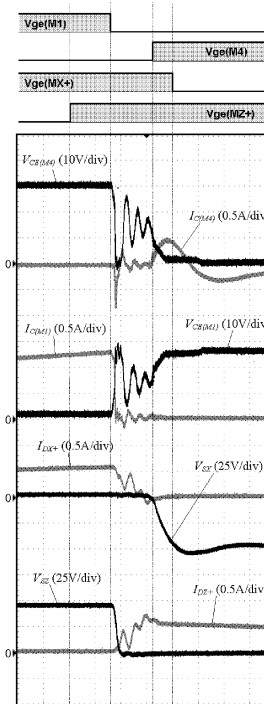


Fig. 8: Switching transient at both stages

## Conclusion

In this paper, a modified natural commutated control HF link inverter topology that consists of a center-tapped transformer and three bidirectional switching arms on the transformer secondary side has been proposed. The main features that improves the power conversion efficiency are summarized as follows:

1. The topology consists of only three bidirectional switching arms to perform natural commutation unipolar SPWM switching scheme. As a result, the conduction loss is reduced.
2. The proposed switching scheme results in the existence of two freewheeling periods per switching cycle.
3. Both inverter and cycloconverter stage operate at soft switching operation.

## References

- [1]. K. Harada, H. Sakamoto, and M. Shoyama, "Phase-controlled DC-AC converter with high-frequency switching," *IEEE Trans. Power Electronics*, vol. 3, pp. 406-411, Oct. 1988.
- [2]. T. Kawabata, K. Honjo, N. Sashida, K. Sanada, and M. Koyama, "High frequency link DC/AC converter with PWM cycloconverter," in *Conf. Rec. of IEEE IAS Conf.*, 1990, pp. 1119-1124, Oct. 1990.
- [3]. P. K. Sood, T. A. Lipo, and I. G. Hansen, "A versatile power converter for high-frequency link systems," *IEEE Trans. Power Electronics*, vol. 3, no. 4, pp. 383 - 390, Oct. 1988.
- [4]. Songquan Deng, Hong Mao, J. Mazumdar, I. Batarseh; K. K. Islam, "A new control scheme for high-frequency link inverter design," in *IEEE APEC '03*, pp. 512 – 517, 9-13 Feb. 2003.
- [5]. M.Z. Ramli, Z. Salam, Leong Soon Toh, Chee Lim Nge, "A bidirectional high-frequency link inverter using center-tapped transformer," in *IEEE 35th Annual PESC 04*, vol. 5, pp. 3883 – 3888, June 2004.
- [6]. H. Fujimoto, K. Kuroki, T. Kagotani, and H. Kidoguchi, "Photovoltaic inverter with a novel cycloconverter for interconnection to a utility line," in *Proc. IEEE IAS'95 Conf.*, vol. 3, pp. 2461-2467, Oct. 1995
- [7]. I. Yamato, N. Tokunaga, Y. Matsuda, Y. Suzuki, and H. Amano, "High frequency link dc-ac converter for UPS with a new voltage clamper," in *IEEE PESC*, pp. 749-756, Jun 1990.
- [8]. M. Matsui, M. Nagai, M. Mochizuki, and A. Nabae, "High-frequency link dc/ac converter with suppressed voltage clamper circuits – naturally commutated phase angle control with self turn-off devices," *IEEE Trans. I.A.*, vol. 32, no. 2, Mar./Apr. 1996.